INTERNATIONAL JOURNAL FOR NUMERICAL METHODS IN FLUIDS, VOL. 9, 385–403 (1989)

UPWIND BASIS FINITE ELEMENTS FOR CONVECTION-DOMINATED PROBLEMS

P. M. STEFFLER

Department of Civil Engineering, University of Alberta, Edmonton, Alberta, Canada T6G 2G7

SUMMARY

Finite elements using higher-order basis functions in the spirit of the QUICK method for convection-dominated fluid flow and transport problems are introduced and demonstrated. Instead of introducing new internal degrees of freedom, completeness is achieved by including functions based on nodal values exterior and upwind to the element domain. Applied with linear test functions to the weak statements for convection-dominated problems, a family of Petrov–Galerkin finite elements is developed. Quadratic and cubic versions are demonstrated for the one-dimensional convection–diffusion test problem. Elements of up to seventh degree are used for local solution refinement. The behaviour of these elements for one-dimensional linear and non-linear advection is investigated. A two-dimensional quadratic upwind element is demonstrated in a streamfunction–vorticity formulation of the Navier–Stokes equations for a driven cavity flow test problem. With some minor reservations, these elements are recommended for further study and application.

KEY WORDS Upwind QUICK Petrov–Galerkin Convection–diffusion Advection Navier–Stokes

INTRODUCTION

Numerical modelling of practical convection-dominated problems arising in fluid mechanics, heat transfer, water resources and other fields has proven difficult. Severe restrictions on mesh or grid spacings associated with centred finite difference or standard Galerkin finite element discretizations are, in general, relaxed through the use of upwind finite differences or Petrov–Galerkin finite elements. The common consequence is the introduction of an artificial or numerical diffusivity, which may cause an excessive loss of solution accuracy.[1, 2] Skew[3] upwind and streamline[4] methods have been devised to limit the artificial diffusion to the flow direction only.

A somewhat different approach is taken in the QUICK (quadratic upwind interpolation for convective kinematics) scheme of Leonard.[5] This method uses a higher-degree upwind-weighted interpolation for the convected quantities at control volume boundaries to obtain a reliable and accurate approximate solution. This method provides a valuable alternative to upwind and skew upwind schemes and has been shown to give better results in certain instances.[6] In other cases, however, skew-upwinding methods have been found to be superior.[7] It appears that the major difficulty with the QUICK method is in its implementation for multidimensional problems. The simple one-dimensional interpolations usually performed appear to give less accurate results and more stability and convergence difficulties for problems in which the flow direction is significantly skewed to the mesh orientation. In addition, the method lacks consistency, with different orders of

0271–2091/89/040385–19$09.50

Received 14 January 1988
Revised 13 June 1988

interpolation applied to the same variable over different boundaries and over the interior of the control volume.

At present there appears to be no analogue in the finite element literature to the QUICK method. It is the purpose of this paper to present a finite element inspired by this approach and demonstrate its behaviour for a few test problems. While based on the idea of upwind interpolation, the proposed method offers the advantages associated with a finite element implementation. Firstly, it allows a consistent treatment of all variables and terms in the governing equations. Secondly, it allows direct generalization to higher dimensions and higher orders of interpolation. Finally, it allows the geometric flexibility of the finite element method. The upwind basis method is therefore not an attempt to duplicate the QUICK scheme in a finite element context but aims rather to exploit the idea of upwind interpolation to its fullest potential.

UPWIND BASIS FUNCTIONS

Most finite element formulations of convection-dominated problems are based on a Petrov–Galerkin approach wherein the test functions $\mathbf{v}(\mathbf{x})$ are upwind-weighted modifications of the basis functions $\mathbf{f}(\mathbf{x})$. The modification is selected to extract a diffusion effect proportional to a measure of the grid spacing in discrete form from the convection terms of the governing equation. The magnitude of the modification, and thus the artificial diffusion, is controlled by one or more arbitrary parameters which may be optimized according to specific criteria.[4,8]

The present study takes a different approach by introducing new, upwind-weighted, *basis functions*. Physically, it is reasonable that the value of a convection-dominated variable within an element should depend more heavily on upstream nodal values than on downstream nodal values. This may be accomplished by increasing the degree of the basis functions. Completeness of the higher-degree polynomial interpolation is attained by slightly relaxing the finite element tradition of purely local basis functions and introducing 'super-local' basis functions which include an effect from a node or nodes external, but close, to the element under consideration. For example, a one-dimensional element spanning the space between two nodes could support a complete quadratic variation over its interior if a third (upwind) nodal value and associated basis function were included. The basis functions for such an element (flow in positive co-ordinate direction) would be similar to those of a standard quadratic element in terms of the local co-ordinate ξ:

$$\mathbf{f}_e(\xi) = \left\{ \begin{array}{c} (3+\xi)(1-\xi)/4 \\ (1+\xi)(3+\xi)/8 \\ -(1-\xi)(1+\xi)/8 \end{array} \right\}; \quad \xi \in (-1, 1). \tag{1}$$

In the same way, cubic basis functions may be developed relying on two additional upwind nodal values:

$$\mathbf{f}_e(\xi) = \left\{ \begin{array}{c} (5+\xi)(3+\xi)(1-\xi)/16 \\ (1+\xi)(3+\xi)(5+\xi)/48 \\ -(1-\xi)(1+\xi)(5+\xi)/16 \\ -(1-\xi)(1+\xi)(3+\xi)/48 \end{array} \right\}; \quad \xi \in (-1, 1). \tag{2}$$

The node ordering and graphical representations of the local functions over an element and global functions for a node are shown in Figure 1.

The upwind basis function concept generalizes easily to even higher-degree elements and higher dimensions.

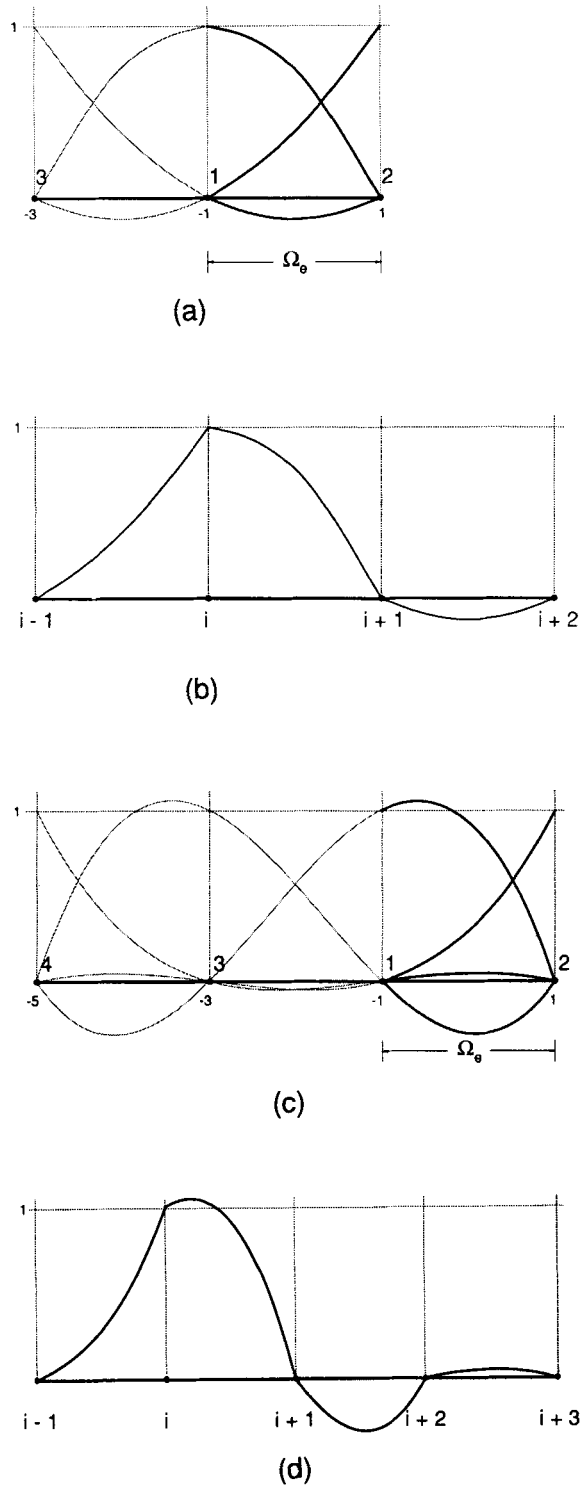

Figure 1. Upwind basis functions: (a) local quadratic; (b) global quadratic; (c) local cubic; (d) global cubic

TEST FUNCTIONS AND DISCRETIZATION OF A MODEL PROBLEM

Several possibilities may be considered for test functions. A Bubnov–Galerkin discretization may be accomplished using the upwind basis functions themselves or, alternatively, the customary linear functions would yield a Petrov–Galerkin approach.

Consider the one-dimensional, steady, convection–diffusion boundary value problem

$$U\frac{\partial\phi}{\partial x}-\frac{\partial}{\partial x}\left(D\frac{\partial\phi}{\partial x}\right)=0, \quad x\in(0, L), \tag{3}$$

$$\phi(x=0)=0, \qquad \phi(x=L)=1,$$

where U is the velocity and D is the diffusivity. Standard weighted residual procedures, using piecewise continuous basis and test functions $\mathbf{f}$ and $\mathbf{v}$, yield the discrete weak statement

$$(\mathbf{C}+\mathbf{K})\mathbf{\Phi}=0, \tag{4}$$

where

$$\mathbf{C}=\int_0^L U\,\mathbf{v}\frac{\mathrm{d}\mathbf{f}}{\mathrm{d}x}\mathrm{d}x, \tag{5}$$

$$\mathbf{K}=\int_0^L D\frac{\mathrm{d}\mathbf{v}}{\mathrm{d}x}\frac{\mathrm{d}\mathbf{f}}{\mathrm{d}x}\mathrm{d}x \tag{6}$$

and

$$\phi_h=\mathbf{f}\mathbf{\Phi} \tag{7}$$

is the approximate solution in terms of nodal values $\mathbf{\Phi}$.

Evaluating the integrals by assembling element contributions is straightforward upon specification of the test functions and the spatial discretization. For the purpose of illustration take U and D as positive constants and elements of equal length h.

For a Bubnov–Galerkin scheme using quadratic upwind functions (QUBG) the element matrices are given in the Appendix. Assembling the jth row of $(\mathbf{C}+\mathbf{K})$ leads to the following discrete equation:

$$\frac{U}{12}(\Phi_{j-2}-8\Phi_{j-1}+8\Phi_{j+1}-\Phi_{j+2})+\frac{D}{12h}(\Phi_{j-2}-16\Phi_{j-1}+30\Phi_j-16\Phi_{j+1}+\Phi_{j+2})=0. \tag{8}$$

The expressions may be recognized as fourth-order centred finite difference representations for the first and second derivatives. Schemes based on such higher-order finite differences have enjoyed some popularity for convection problems, and the present formulation adds finite element advantages of geometric flexibility and boundary condition handling (at outflow boundaries at least). They still suffer, however, from the unreliability of any centred formulation.

A Petrov–Galerkin family of elements may also be defined by using standard linear test functions. In this case only two test functions are non-zero over an element (of any degree) while the number of basis functions varies, resulting in non-square element matrices (Appendix). For the quadratic upwind basis (QUPG), assembling one row of the global matrices as above results in the following equation:

$$\frac{U}{12}(\Phi_{j-2}-9\Phi_{j-1}+3\Phi_j+5\Phi_{j+1})+\frac{D}{h}(-\Phi_{j-1}+2\Phi_j-\Phi_{j+1})=0. \tag{9}$$

For the cubic upwind basis functions (CUPG) the following discrete equation is obtained:

$$\frac{U}{24}(-\Phi_{j-3}+6\Phi_{j-2}-24\Phi_{j-1}+10\Phi_j+9\Phi_{j+1})+\frac{D}{h}(-\Phi_{j-1}+2\Phi_j-\Phi_{j+1})=0. \tag{10}$$

The diffusion terms are unaffected compared with a standard linear finite element formulation, while a Taylor series expansion of the convection terms reveals that both methods give second-order-accurate approximations for the first derivative. Combining the Taylor series expansions for the individual terms gives the actual differential equation modelled by the QUPG discretization:

$$U\frac{\partial\phi_h}{\partial x}-D\frac{\partial^2\phi_h}{\partial x^2}+\frac{h^2}{12}\frac{\partial^2}{\partial x^2}\left(U\frac{\partial\phi_h}{\partial x}-D\frac{\partial^2\phi_h}{\partial x^2}\right)$$
$$+\frac{h^3}{12}U\frac{\partial^4\phi_h}{\partial x^4}+\frac{h^4}{720}\left(9U\frac{\partial^5\phi_h}{\partial x^5}-2D\frac{\partial^6\phi_h}{\partial x^6}\right)+O(h^5)=0. \tag{11}$$

The equation modelled by the CUPG scheme is

$$U\frac{\partial\phi_h}{\partial x}-D\frac{\partial^2\phi_h}{\partial x^2}+\frac{h^2}{12}\frac{\partial^2}{\partial x^2}\left(U\frac{\partial\phi_h}{\partial x}-D\frac{\partial^2\phi_h}{\partial x^2}\right)+\frac{h^4}{720}\left(21U\frac{\partial^5\phi_h}{\partial x^5}-2D\frac{\partial^6\phi_h}{\partial x^6}\right)+O(h^5)=0. \tag{12}$$

As may be observed by recursive substitution, the QUPG method gives an overall third-order-accurate discretization while the CUPG scheme is fourth-order-accurate.

A comparison with the QUICK algorithm is of interest at this point. Using quadratic upwind interpolation for the convective flux of ϕ at the control volume boundaries[5] under the same set of conditions as above, the following discrete equation is obtained:

$$\frac{U}{8h}(\Phi_{j-2}-7\Phi_{j-1}+3\Phi_j+(^j{}_{+1})+\frac{D}{h^2}(-\Phi_{j-1}+2\Phi_j-\Phi_{j+1})=0. \tag{13}$$

The modelled equation is then

$$U\frac{\partial\phi_h}{\partial x}-D\frac{\partial^2\phi_h}{\partial x^2}+\frac{h^2}{12}\frac{\partial^2}{\partial x^2}\left(U\frac{\partial\phi_h}{\partial x}-D\frac{\partial^2\phi_h}{\partial x^2}\right)-\frac{h^2}{24}U\frac{\partial^3\phi_h}{\partial x^3}$$
$$+\frac{h^3}{16}U\frac{\partial^4\phi_h}{\partial x^4}+\frac{h^4}{1440}\left(-33U\frac{\partial^5\phi_h}{\partial x^5}-4D\frac{\partial^6\phi_h}{\partial x^6}\right)+O(h^5)=0. \tag{14}$$

The QUICK method is therefore of second-order accuracy overall. Differing signs on the second- and third-order error terms indicate partial cancellation and higher-order accuracy near a cell Peclet number of 2/3.

An alternative form of the QUICK algorithm proposed by Leonard[2] uses a third-order-accurate expression for the first derivative over the same four nodes:

$$\frac{U}{6h}(\Phi_{j-2}-6\Phi_{j-1}+3\Phi_j+2\Phi_{j+1})+\frac{D}{h^2}(-\Phi_{j-1}+2\Phi_j-\Phi_{j+1})=0. \tag{15}$$

The modelled equation for this case is

$$U\frac{\partial\phi_h}{\partial x}-D\frac{\partial^2\phi_h}{\partial x^2}+\frac{h^2}{12}\frac{\partial^2}{\partial x^2}\left(U\frac{\partial\phi_h}{\partial x}-D\frac{\partial^2\phi_h}{\partial x^2}\right)-\frac{h^2}{12}U\frac{\partial^3\phi_h}{\partial x^3}$$
$$+\frac{h^3}{12}U\frac{\partial^4\phi_h}{\partial x^4}+\frac{h^4}{360}\left(-12U\frac{\partial^5\phi_h}{\partial x^5}-D\frac{\partial^6\phi_h}{\partial x^6}\right)+O(h^5)=0. \tag{16}$$

Despite the improvement in the accuracy of the convective term, the method is only of second-order accuracy overall. In fact, the leading error term is twice as large as for the first QUICK scheme. Cancellation and fourth-order accuracy near a cell Peclet number of unity are predicted in this case.

Convergence in the L_2 norm of these methods for the above convection–diffusion problem is shown in Figure 2(a). The overall Peclet number ($Pe \equiv UL/D$) is 1000. N is the number of nodes used in the discretization and the L_2 norm is calculated by numerical integration of

$$\|\mathbf{e}\|_{L_2} = \left(\int_0^1 (\phi - \phi_h)^2 \, dx \right)^{1/2}, \tag{17}$$

with ϕ given by the analytical solution.

For the QUPG method the upstream boundary is handled with a single linear Galerkin element, and for the CUPG scheme the first element is a linear Galerkin element and the second element is a QUPG element. Note that no special treatments are required at the downstream boundary. Standard linear Galerkin (LG), quadratic Galerkin (QG) and optimal (exact nodal values) Petrov–Galerkin (PG) are also shown for comparison. Figure 2(b) shows the convergence of the maximum error in nodal values (except for Petrov–Galerkin) and also includes the first mentioned QUICK scheme.

The orders of accuracy derived above are confirmed by the convergence rates of the maximum nodal error. The local 'superconvergence' of the QUICK method is also confirmed. The asymptotic convergence rates of the QUPG and CUPG methods in the L_2 norm are also confirmed to be commensurate with the degree of the respective basis functions. More importantly perhaps, the error remains limited for large element Peclet number ($Pe_h \equiv Uh/D$). At $N = 10$ ($Pe_h = 100$) the L_2 error norms for the PG, QUPG and CUPG methods are 0·1820, 0·1764 and 0·1426 respectively. The form of the QUPG and CUPG solutions for this discretization is shown in Figure 3.

The computed values oscillate but the magnitude and extent of the oscillations are limited. The upwind finite element method appears to provide reliable solutions to this simple but very demanding problem, while improving rather than degrading the order of accuracy and convergence compared to the Galerkin method. In particular no artificial diffusion in the form of a first-order (in h) truncation error has been introduced.

SOLUTION REFINEMENT USING HIGHER-ORDER UPWIND ELEMENTS

The upwind (or otherwise extended) basis finite elements offer an interesting possibility for solution refinement. The degree of the polynomial approximation for an element may be increased by incorporating more externally based functions. It should be possible to obtain better solutions by locally increasing the order of approximation in regions of rapid change without increasing the number of unknowns to be solved for. Only the local bandwidth or profile height of the global matrices would change. Extra computational effort would be minimal. Iterative refinement methods using the previously factored matrix could be easily devised.

The effectiveness of this approach is indicated by the results of a numerical experiment shown in Table I. The problem is as above with $Pe = 1000$ and $N = 40$. All elements except the last are linear Galerkin elements. The last element is a successively higher (up to seventh) degree upwind basis element.

Figure 4 shows graphically the improvement in the approximate solution obtained.

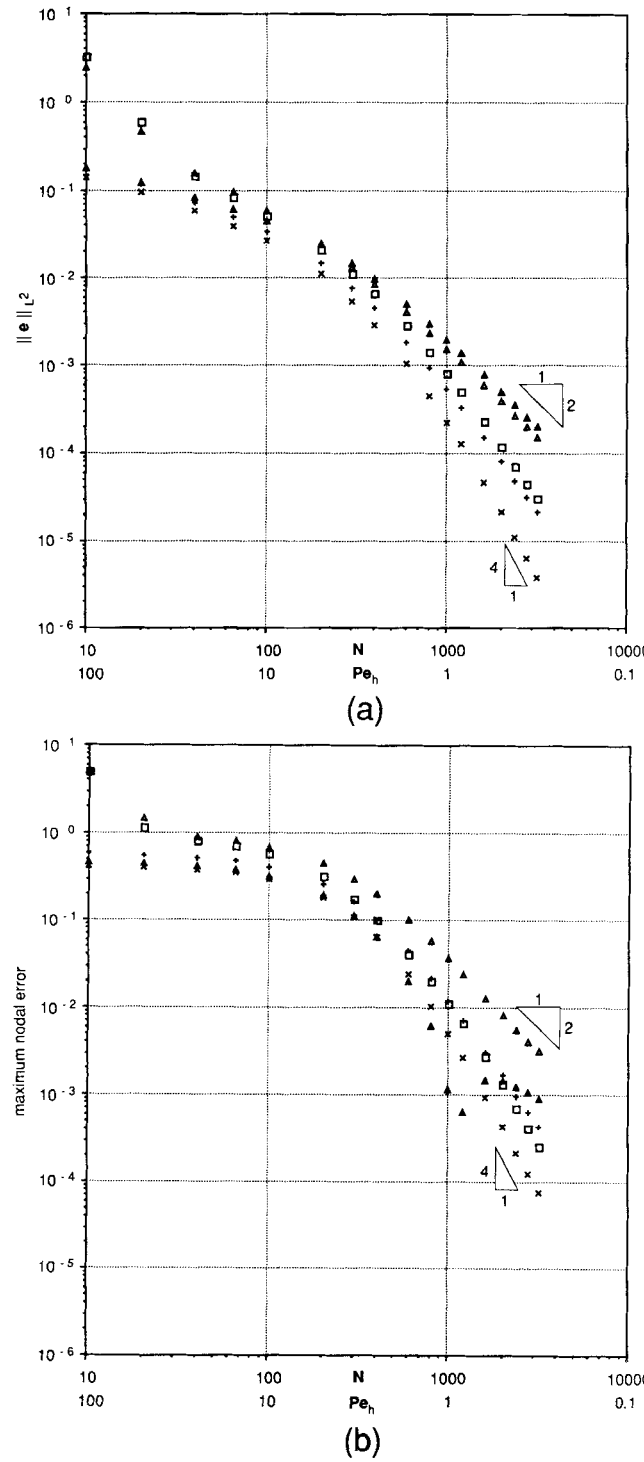

Figure 2. Convergence for one-dimensional convection–diffusion test problem: (a) in L_2 norm; (b) in maximum nodal error. Key: △, LG; □, QG; ▲, (a) PG or (b) QUICK; +, QUPG; ×, CUPG

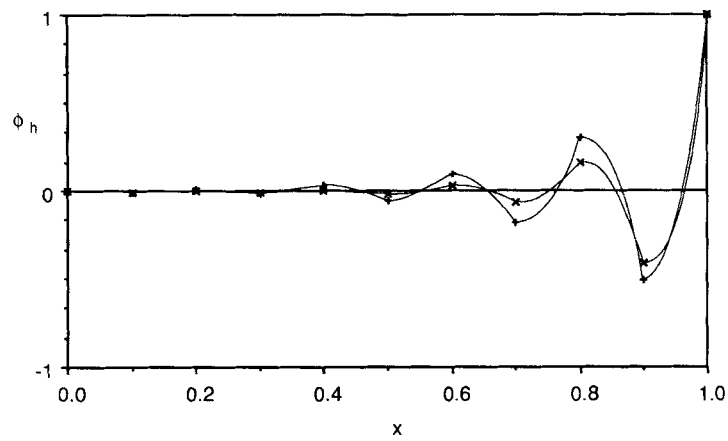

Figure 3. Quadratic and cubic upwind solutions for the one-dimensional convection–diffusion test problem; $Pe_h = 100$. Key: +, QUPG; ×, CUPG

Table I. Effect of higher-degree elements

	Error	
Degree of last element	in L_2 norm	max. nodal error
1 (LG)	0·1588	0·855
2 (QUPG)	0·0989	0·486
3 (CUPG)	0·0730	0·323
4	0·0579	0·225
5	0·0480	0·159
6	0·0413	0·111
7	0·0367	0·076

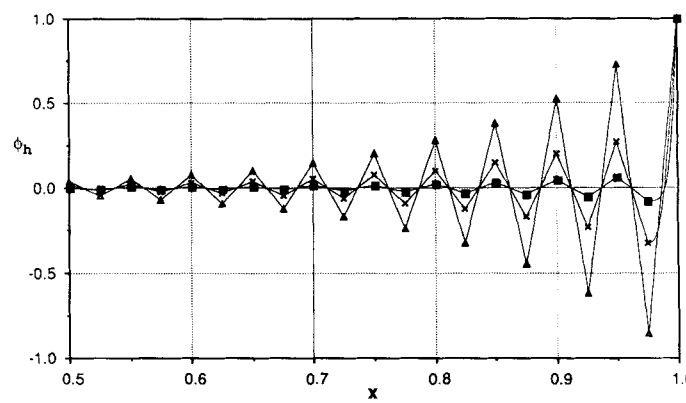

Figure 4. Effect of using higher-degree basis elements; $Pe_h = 25$. Degree of last element: △, 1; ×, 3; ■, 7

LINEAR ADVECTION

The finite element method applied in a consistent way to transient problems, in contrast to most finite difference and finite volume methods, results in non-diagonal mass and capacity matrices. This leads to improved accuracy in the modelling of advective phenomena in particular. In this section the use of a consistent formulation for transient advection problems based on upwind elements is demonstrated.

Consider one-dimensional advection of a single scalar quantity $\phi(x, t)$ at a constant (positive) velocity U, modelled by the following problem:

$$\frac{\partial \phi}{\partial t} + U \frac{\partial \phi}{\partial x} = 0, \qquad \phi(x, 0) = \phi_0(x) \tag{18}$$

and periodic boundary conditions. The exact solution at any time t is simply a translation of $\phi_0(x)$ a distance of Ut. Any numerical dissipation introduced by the computational scheme will appear as a damping of the original profile. Dispersion errors will also occur as the shorter Fourier components of the original profile propagate at incorrect phase velocities.

Standard procedures applied to equation (18) over the domain Ω yield the semidiscrete weak statement

$$\mathbf{M} \frac{\mathrm{d}\boldsymbol{\Phi}}{\mathrm{d}t} + \mathbf{C}\boldsymbol{\Phi} = 0, \tag{19}$$

where

$$\mathbf{M} = \int_0^L \mathbf{v}\mathbf{f}\,\mathrm{d}x, \tag{20}$$

$\mathbf{C}$ is as defined in equation (5) and $\phi_h(x, t) = \mathbf{f}(x)\,\boldsymbol{\Phi}(t)$. $\mathbf{M}$ may be calculated by assembly of the element matrices (Appendix). The actual equations modelled by the semidiscrete equation above are as follows:

$$\frac{\partial \phi_h}{\partial t} + U \frac{\partial \phi_h}{\partial x} + \frac{h^2}{12} \frac{\partial^2}{\partial x^2}\left(\frac{\partial \phi_h}{\partial t} + U \frac{\partial \phi_h}{\partial x}\right) + \frac{h^3}{24} \frac{\partial^3}{\partial x^3}\left(\frac{\partial \phi_h}{\partial t} + U \frac{\partial \phi_h}{\partial x}\right)$$
$$- \frac{h^4}{72} \frac{\partial^4}{\partial x^4}\left(\frac{\partial \phi_h}{\partial t} + U \frac{\partial \phi_h}{\partial x}\right) + \frac{h^4}{720} U \frac{\partial^5 \phi_h}{\partial x^5} + O(h^5) = 0 \tag{21}$$

for the QUPG discretization and

$$\frac{\partial \phi_h}{\partial t} + U \frac{\partial \phi_h}{\partial x} + \frac{h^2}{12} \frac{\partial^2}{\partial x^2}\left(\frac{\partial \phi_h}{\partial t} + U \frac{\partial \phi_h}{\partial x}\right) + \frac{7h^4}{240} \frac{\partial^4}{\partial x^4}\left(\frac{\partial \phi_h}{\partial t} + U \frac{\partial \phi_h}{\partial x}\right)$$
$$- \frac{h^5}{45} \frac{\partial^5}{\partial x^5}\left(\frac{\partial \phi_h}{\partial t} + U \frac{\partial \phi_h}{\partial x}\right) + \frac{h^5}{720} U \frac{\partial^6 \phi_h}{\partial x^6} + O(h^6) = 0 \tag{22}$$

for the CUPG discretization. Recursive substitution indicates fourth- and fifth-order accuracies for the respective semidiscrete schemes. It is well known that a similar analysis applied to a linear Galerkin formulation also leads to a fourth-order-accurate semidiscrete algorithm. The leading error term, however, is four times as large as that for the QUPG method.

Specification of a time integration algorithm for the solution of the ordinary differential equations is required to complete the formulation of this test problem. For comparison purposes a trapezoidal rule (Crank–Nicolson) implicit method will be used. Figure 5 shows the dissipation and dispersion ratios (numerical/exact) as a function of discretization (N_λ = number of nodes per

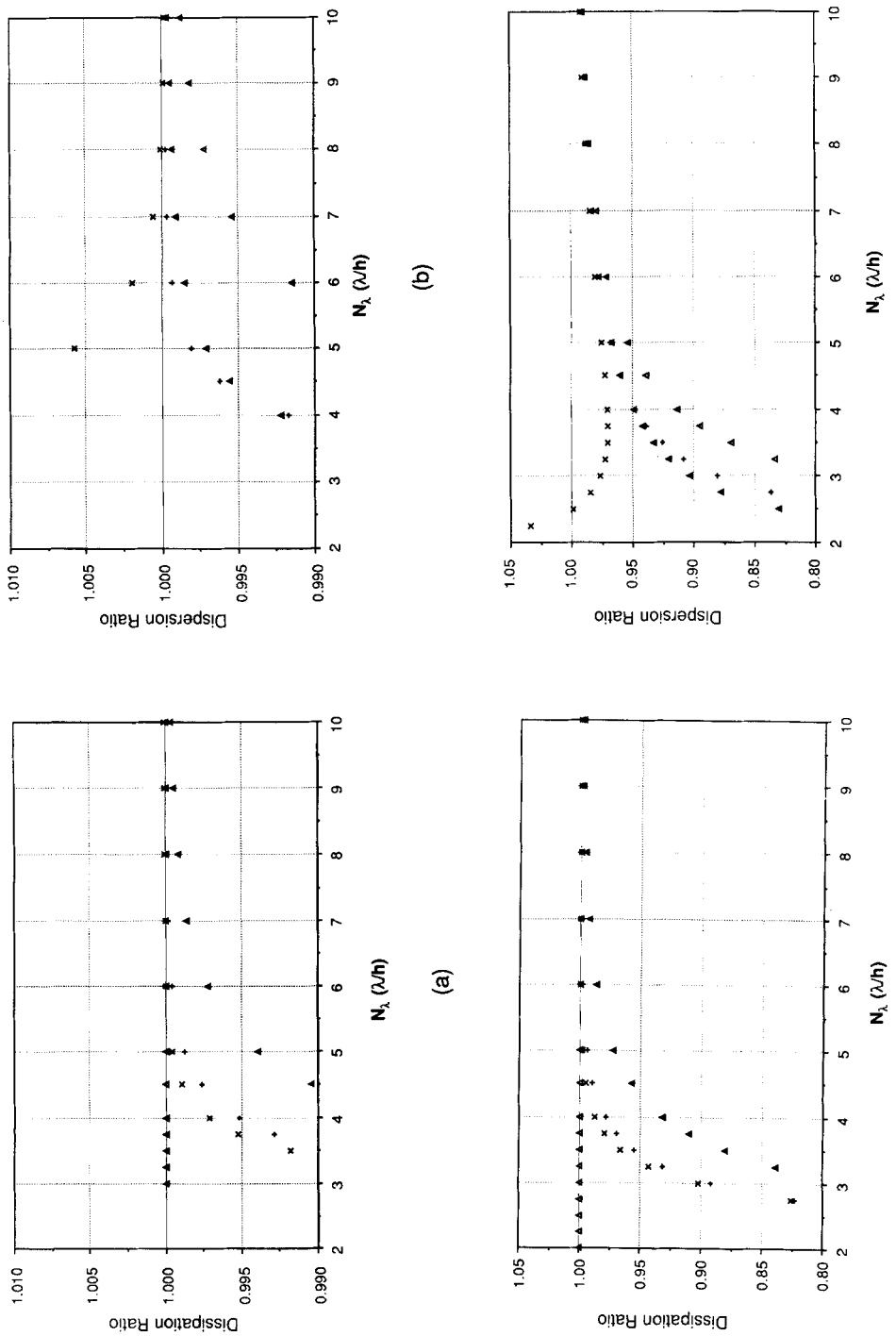

Figure 5. Propagation characteristics for one-dimensional advection using trapezoidal rule time integration: (a) dissipation ratio, $Cr = 0{\cdot}1$; (b) dispersion ratio, $Cr = 0{\cdot}1$; (c) dissipation ratio, $Cr = 0{\cdot}5$; (d) dispersion ratio, $Cr = 0{\cdot}5$. Key: △, LG; ▲, PG; +, QUPG; ×CUPG

wavelength) obtained from a Fourier modal analysis of the resulting recursion relations at Courant numbers ($Cr \equiv U\Delta t/h$) of 0·1 and 0·5. Analysis of the QUPG and CUPG methods is straightforward since all nodes are treated identically (in contrast to the usual higher-order elements). Results for the linear Bubnov–Galerkin (LG) scheme and a consistent Petrov–Galerkin (PG) method with upwind weighting set to 0·25 and trapezoidal rule time integration are also shown for comparison.

The particular choice of upstream weighting for the Petrov–Galerkin method (very close to the optimal semidiscrete value of $1/\sqrt{15}$) gives essentially equivalent dispersion to the QUPG scheme. The dissipation of the QUPG method is, however, more selective, preserving the four- to ten-node wavelengths longer. The QUPG method is definitely superior to the linear Galerkin method, providing better dispersion characteristics and dissipation of shortest wave components. The CUPG scheme shows modest improvement over the QUPG method in both dissipation and dispersion.

Figure 6 shows the results of application of the above four schemes to an advection test problem at $Cr = 0{\cdot}24$. These results confirm the conclusions of the Fourier analysis. The CUPG method in particular gives a peak reduction of less than 5%.

To take advantage of the high-order accuracy inherent in the semidiscrete scheme, a high-order temporal discretization should be used. Second-order-accurate temporal schemes such as Crank–Nicolson are suboptimal for even linear finite element spatial discretizations. Higher-order time-stepping schemes such as the Euler–Taylor–Galerkin (ETG)[9] or Euler–characteristic–Galerkin (ECG)[10] have been devised with remarkable improvements in performance. An analogous set of high-order algorithms should be possible based on the QUPG and CUPG discretizations. It is interesting that the QUPG method naturally incorporates the upstream node and third-order spatial difference that appears in the Taylor weak statement formulation.[11] The element matrix for

$$\mathbf{S} = \int_{\Omega} \frac{d\mathbf{v}}{dx} \frac{d^2\mathbf{f}}{dx^2} d\Omega \tag{23}$$

is included in the Appendix.

NON-LINEAR ADVECTION–DIFFUSION

A convenient test problem for the evaluation of numerical schemes intended for fluid mechanics applications is Burger's equation:

$$\frac{\partial u}{\partial t} + u\frac{\partial u}{\partial x} - \frac{\partial}{\partial x}\left(D\frac{\partial u}{\partial x}\right) = 0. \tag{24}$$

This equation may lead to shock (in the sense of a gradient steeper than the mesh can display) type solutions as the element Reynolds number ($Re_h = uh/D$) becomes large. The propagation velocity of such a shock is simply the average of the upstream and downstream velocities u_1 and u_2. In particular, if the magnitudes of u_1 and u_2 are equal and the directions are opposite, a stationary shock will result. Figures 7(a) and 7(b) show the steady state solution obtained for the initial and boundary conditions

$$u(x, t=0) = \begin{cases} 1, & 0 \le x \le 0{\cdot}5 \\ -1, & 0{\cdot}51 \le x \le 1, \end{cases}$$

$$u(0, t) = 1, \qquad u(1, t) = -1,$$

using QUPG and CUPG elements ($h = 0{\cdot}1$) respectively.

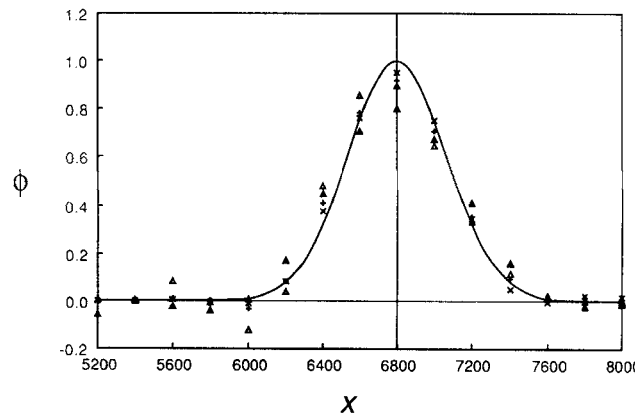

Figure 6. Advection test problem results; $U=0{\cdot}5$, $h=200$, $\Delta t=96$, $t=9600$. Key: △, LG; ▲, PG; +, QUPG, × CUPG

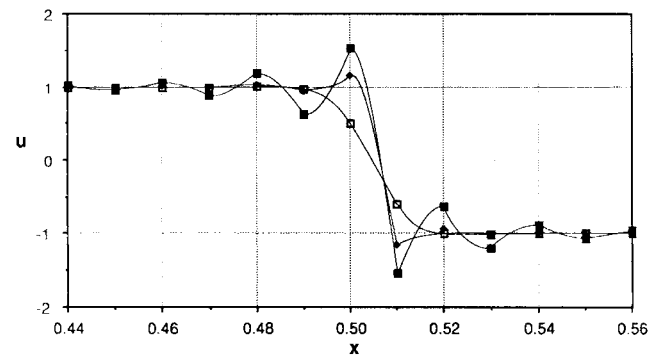

(a)

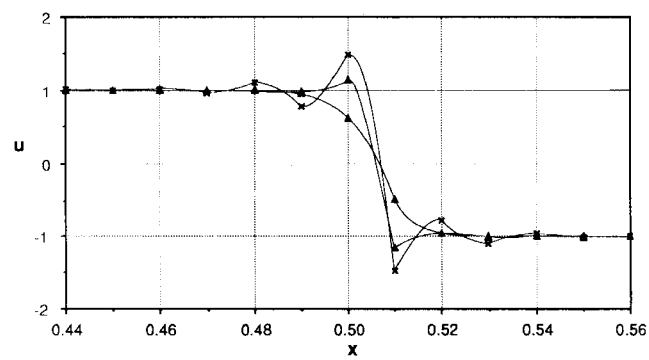

(b)

Figure 7. Solutions of non-linear steady state advection–diffusion test problem—(a) QUPG: □, $Re_h=2{\cdot}5$; ◆, $Re_h=10$; ■, $Re_h=\infty$; (b) CUPG; △, $Re_h=2{\cdot}5$; ▲, $Re_h=10$; ×, $Re_h=\infty$

These methods capture the shock but, as might be expected from Figure 3, do not give monotonic solutions for large element Reynolds numbers. The disturbance created is, however, limited in magnitude and, especially for the cubic basis, is dissipated very quickly away from the shock.

A FLUID FLOW APPLICATION

Generalization of the upwind basis elements to higher dimensions and more complicated and interesting problems is straightforward. As a demonstration consider a streamfunction–vorticity formulation of two-dimensional incompressible flow of a viscous fluid. The equations are

$$\frac{\partial^2\psi}{\partial x^2}+\frac{\partial^2\psi}{\partial y^2}=-\omega, \tag{25}$$

$$\frac{\partial\psi}{\partial y}\frac{\partial\omega}{\partial x}-\frac{\partial\psi}{\partial x}\frac{\partial\omega}{\partial y}=\frac{\partial}{\partial x}\left(\nu\frac{\partial\omega}{\partial x}\right)+\frac{\partial}{\partial y}\left(\nu\frac{\partial\omega}{\partial y}\right), \tag{26}$$

where ψ is the streamfunction which is related to the velocity components u and v by

$$u=\partial\psi/\partial y, \qquad v=-\partial\psi/\partial x, \tag{27}$$

and ω is the vorticity given by

$$\omega=\frac{\partial v}{\partial x}-\frac{\partial u}{\partial y}. \tag{28}$$

A popular problem for which solutions are available and which tests the performance of a method in a recirculating flow is the driven cavity problem. The domain is square with sides of unit length and the appropriate boundary conditions are

$$\psi=0, \qquad \omega=-\partial^2\psi/\partial n^2 \tag{29}$$

on all sides with n the inward normal direction. Since the present calculation is restricted to a regular orthogonal mesh, the latter boundary condition is reasonably well approximated by

$$\omega_o=\frac{3}{h^2}(\psi_b-\psi_i)-\frac{3U}{h}-\frac{\omega_i}{2}, \tag{30}$$

where the subscript 'b' denotes a boundary nodal value and the subscript 'i' denotes the value at the first inside node (distance of h normal to the boundary). U is the tangential boundary velocity which is zero on the bottom and sides and unity on the top of the cavity. At the top corners the value is undetermined.

The two-dimensional QUPG shape functions were developed simply as tensor products of the one-dimensional functions. The elements used are shown in Figure 8.

The nine-node element combines quadratic functions in both directions, while the six-node element (used where the flow direction is away from a boundary) uses linear functions in the short direction. Test functions are the standard two-dimensional chapeau functions. The upwinding direction is determined from differences of ψ along the element sides and the element node orderings are rotated accordingly. No attempt is made to insure inter-element continuity along lines of flow direction change.

A uniform mesh of 20 by 20 elements and a mesh of 21 by 21 elements of size graded by a geometric factor of 1·2 increasing away from the sides were used. The graded mesh calculation was intended to reduce the adverse effects of the vorticity boundary condition and the presence of

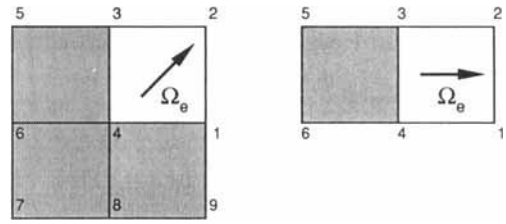

Figure 8. Two-dimensional quadratic upwind elements

lower-order elements on parts of the boundary, and to attempt to resolve the thin boundary layers present. Isoparametric mapping was used for the graded mesh. Some care was therefore required in the mesh gradation (similar to selection of internal node location in conventional finite elements). Contour plots of vorticity and streamfunction for $Re = 1000$ on the graded mesh are shown in Figure 9.

The contouring was performed element by element using the actual upwind basis functions. Minor discontinuities are noticeable at points of flow direction change, especially near steep gradients.

The vortex centre values are compared with the results of Schreiber and Keller[12] in Table II and are found to be in good agreement, especially for the graded mesh. The reference values were obtained from a finite difference solution on a grid of 141 by 141 lines, except for the primary vortex values which were obtained by Richardson extrapolation of a sequence of grids (100, 120 and 141 lines in each direction).

The above results were obtained using $U = 1/2$ at the top corners. Very little effect was observed by changing this. Figures 10(a) and 10(b) show a detail of the top right corner of the graded mesh for $U = 1/2$ and $U = 0$ respectively. The nodal values of vorticity are shown superimposed on the streamfunction contours.

Only the vorticity values very close to the corner are significantly affected, while the streamfunction contours are virtually identical. For comparison a detail of the top corner of the uniform mesh is also shown in Figure 10(c). The larger spacing has clearly affected the accuracy of the boundary vorticity values, and significant oscillation of the vorticity values is evident in the corner impingement region. The streamfunction contours remain quite reasonable, however.

COMPUTATIONAL ASPECTS

The concept of local shape and test functions is considered fundamental to the finite element method. It may seem that the introduction of non-local functions would violate some essential premise and invalidate the approach. It should be remembered, however, that the finite element method is distinguished among general weighted residual methods by its computability. That is, the locality of the functions is essentially a convenience. In this regard, the proposed 'super-local' basis functions are easily accommodated. The program used for these test problems was an existing finite element code modified only to include new element matrix and connectivity table generation routines. No less would be required for any new element.

Since the equation solver used (LU decomposition, profile storage) assumes a symmetric matrix profile, element matrices were padded with zeros to make them square. Storage and execution times experienced are therefore not indicative of the minimum cost of the method. Indeed, since the dot products performed in an LU decomposition are of a length equal to the shorter of the

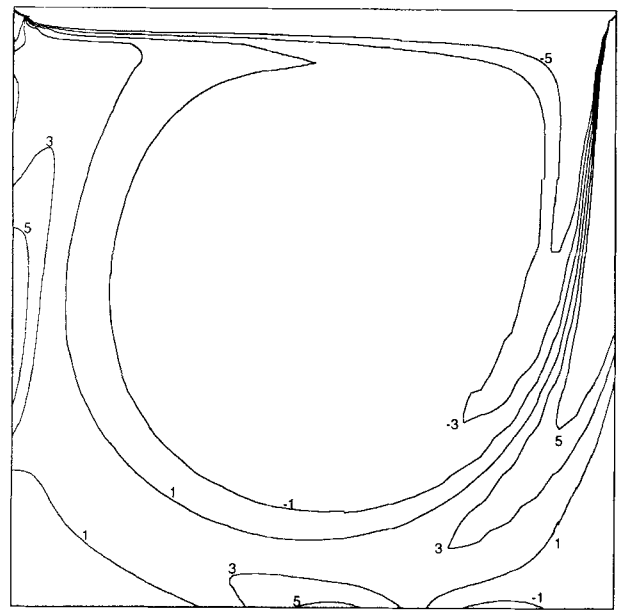

(a)

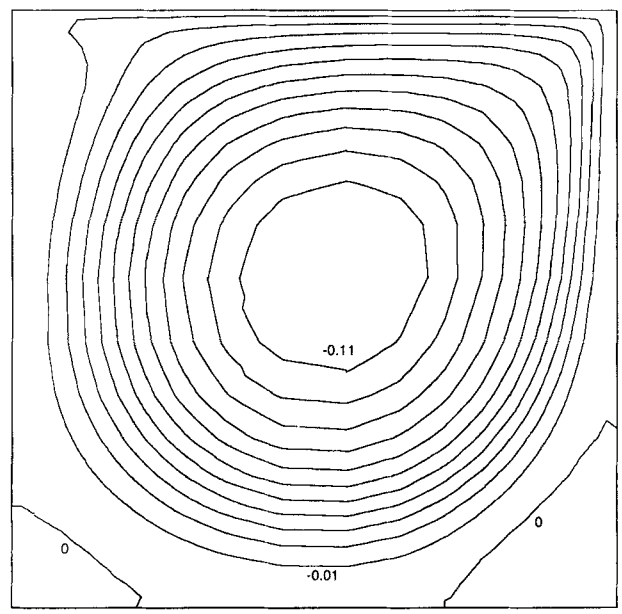

(b)

Figure 9. Driven cavity solution for $Re = 1000$ by quadratic upwind elements: (a) vorticity; (b) streamfunction

column and row involved, the potential time savings resulting from considering the non-symmetric profile may be significant. This would be especially true for higher-order elements and higher dimensions.

CONCLUSIONS

Upwind basis finite elements have been presented and have been shown to give good results for a number of convection-dominated test problems. As indicated by the L_2 norm, these elements emphasize and take full advantage of the basic finite element premise of consistent, piecewise functional solution approximation. By contrast, in application, they act somewhat like a finite difference method, requiring special treatment at some boundaries and working best and most conveniently on regular, carefully graded meshes.

Table II. Driven cavity vortex centre value comparison

Vortex		QUPG (graded)	QUPG (uniform)	Ref. 12
Primary	ψ	−0·1228	−0·1265	−0·1189
(centre)	ω	−2·058	−2·194	−2·068
Secondary	ψ	0·00169	0·00119	0·00170
(lower right)	ω	1·058	0·695	0·999
Tertiary	ψ	0·00028	0·00020	0·00022
(lower left)	ω	0·587	0·231	0·302

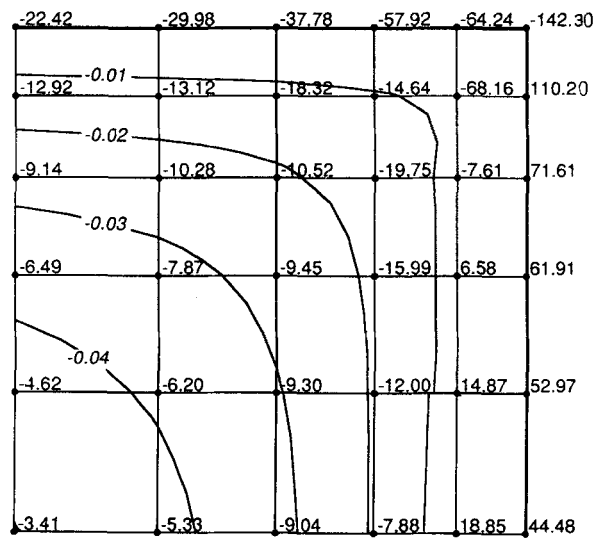

(a)

Fig. 10(a)

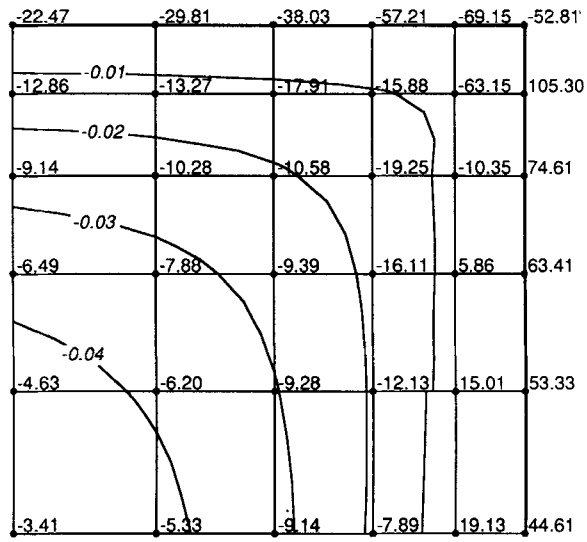

(b)

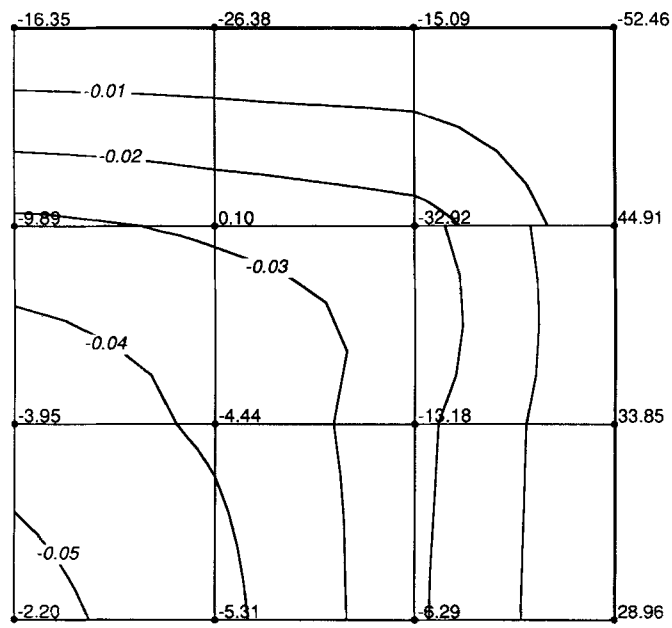

(c)

Figure 10. Detail of top right corner of driven cavity solutions for $Re = 1000$ by quadratic upwind elements: (a) $U = 1/2$; (b) $U = 0$; (c) uniform mesh, $U = 1/2$.

In contrast to the QUICK method, the idea of upwind interpolation is applied consistently to all terms of the governing equation. Solutions to transient problems in particular benefit from this approach.

In contrast to most Petrov–Galerkin methods, there are no upwinding parameters introduced. All that is required is the flow direction for a particular element. While this reduces the possibility of 'tuning' a solution, it simplifies application from a user's perspective.

The elements introduced are more computationally expensive than linear Galerkin and Petrov–Galerkin elements but are less expensive than the equivalent higher-order elements, especially if optimized methods are used. The greatest utility of these elements may lie in refinement (local or global) of coarse mesh solutions. The discretization would remain the same but the connectivity and nodal coupling would increase.

Broader application of 'super-local' shape functions should be investigated. For problems not dominated by convective effects, the fourth-order finite differences resulting from use of the quadratic upwind basis in a Galerkin formulation are interesting and encouraging. Such methods may provide insights into the relationships between finite difference and finite element methods.

Although many questions, especially those of reliability and efficiency, remain to be answered, upwind basis elements may provide a useful alternative in practical modelling applications.

APPENDIX: ELEMENT MATRICES

The one-dimensional element matrices used in the analysis of the upwind basis finite elements are listed below. They are defined in terms of the element test functions $\mathbf{v}_e$ and basis functions $\mathbf{f}_e$ as

$$\mathbf{M}_e = \int_{-1}^{1} \mathbf{v}_e \mathbf{f}_e \, d\xi, \tag{31}$$

$$\mathbf{C}_e = \int_{-1}^{1} \mathbf{v}_e \frac{d\mathbf{f}_e}{d\xi} d\xi, \tag{32}$$

$$\mathbf{K}_e = \int_{-1}^{1} \frac{d\mathbf{v}_e}{d\xi} \frac{d\mathbf{f}_e}{d\xi} d\xi, \tag{33}$$

$$\mathbf{S}_e = \int_{-1}^{1} \frac{d\mathbf{v}_e}{d\xi} \frac{d^2\mathbf{f}_e}{d\xi^2} d\xi. \tag{34}$$

Quadratic upwind Bubnov–Galerkin

$$\mathbf{M}_e = \frac{1}{6}\begin{bmatrix} 0 & 0 & 0 \\ 0 & 2 & 1 \\ 0 & 1 & 2 \end{bmatrix} + \frac{1}{120}\begin{bmatrix} 1 & -7 & -4 \\ -7 & 24 & 3 \\ -4 & 3 & -9 \end{bmatrix}, \tag{35}$$

$$\mathbf{C}_e = \frac{1}{2}\begin{bmatrix} 0 & 0 & 0 \\ 0 & -1 & 1 \\ 0 & -1 & 1 \end{bmatrix} + \frac{1}{12}\begin{bmatrix} 0 & 1 & -1 \\ -1 & 0 & 1 \\ 1 & -1 & 0 \end{bmatrix}, \tag{36}$$

$$\mathbf{K}_e = \begin{bmatrix} 0 & 0 & 0 \\ 0 & 1 & -1 \\ 0 & -1 & 1 \end{bmatrix} + \frac{1}{12}\begin{bmatrix} 1 & -2 & 1 \\ -2 & 4 & -2 \\ 1 & -2 & 1 \end{bmatrix}. \tag{37}$$

Quadratic upwind Petrov–Galerkin

$$\mathbf{M}_e=\frac{1}{6}\begin{bmatrix}0&2&1\\0&1&2\end{bmatrix}+\frac{1}{24}\begin{bmatrix}-1&2&-1\\-1&2&-1\end{bmatrix}, \tag{38}$$

$$\mathbf{C}_e=\frac{1}{2}\begin{bmatrix}0&-1&1\\0&-1&1\end{bmatrix}+\frac{1}{12}\begin{bmatrix}-1&2&-1\\1&-2&1\end{bmatrix}, \tag{39}$$

$$\mathbf{K}_e=\begin{bmatrix}0&1&-1\\0&-1&1\end{bmatrix}, \tag{40}$$

$$\mathbf{S}_e=\begin{bmatrix}-1&2&-1\\1&-2&1\end{bmatrix}. \tag{41}$$

Cubic upwind Petrov–Galerkin

$$\mathbf{M}_e=\frac{1}{6}\begin{bmatrix}0&0&2&1\\0&0&1&2\end{bmatrix}+\frac{1}{24}\begin{bmatrix}0&-1&2&-1\\0&-1&2&-1\end{bmatrix}+\frac{1}{360}\begin{bmatrix}7&-21&21&-7\\8&-24&24&-8\end{bmatrix}, \tag{42}$$

$$\mathbf{C}_e=\frac{1}{2}\begin{bmatrix}0&0&-1&1\\0&0&-1&1\end{bmatrix}+\frac{1}{12}\begin{bmatrix}0&-1&2&-1\\0&1&-2&1\end{bmatrix}+\frac{1}{24}\begin{bmatrix}1&-3&3&-1\\-1&3&-3&1\end{bmatrix}, \tag{43}$$

$$\mathbf{K}_e=\begin{bmatrix}0&0&1&-1\\0&0&-1&1\end{bmatrix}. \tag{44}$$

REFERENCES

1. P. M. Gresho and R. L. Lee, 'Don't suppress the wiggles—they are telling you something!', in T. J. R. Hughes (ed.), *Finite Element Methods for Convection Dominated Flows*, ASME, AMD-34, New York, 1979, pp. 37–61.
2. B. P. Leonard, 'A survey of finite differences of opinion on numerical muddling of the incomprehensible defective confusion equation', in T. J. R. Hughes (ed.), *Finite Element Methods for Convection Dominated Flows*, ASME, AMD-34, New York, 1979, pp. 1–10.
3. G. D. Raithby, 'Skew upstream differencing schemes for problems involving fluid flow', *J. Comput. Methods Appl. Mech. Eng.*, **9**, 153–164 (1976).
4. A. N. Brooks and T. J. R. Hughes, 'A multidimensional upwind scheme with no crosswind diffusion', *J. Comput. Methods Appl. Mech. Eng.*, **32**, 199–259 (1982).
5. B. P. Leonard, 'A stable and accurate convective modelling procedure based on quadratic upstream interpolation', *J. Comput. Methods Appl. Mech. Eng.*, **19**, 59–98 (1979).
6. P. G. Huang, B. E. Launder and M. A. Leschziner, 'Discretization of non-linear convection processes: a broad-range comparison of four schemes', *J. Comput. Methods Appl. Mech. Eng.*, **48**, 1–24 (1985).
7. M. A. R. Sharif and A. A. Busnaina, 'Assessment of finite difference approximations in the simulation of practical flow problems', *AIAA 24th Aerospace Meeting*, Reno, Nevada, 1986.
8. T. E. Tezduyar and D. K. Ganjoo, 'Petrov–Galerkin formulations with weighting functions dependent upon spatial and temporal discretization: applications to transient convection–diffusion problems', *J. Comput. Methods Appl. Mech. Eng.*, **59**, 49–71 (1986).
9. V. Selmin, J. Donea and L. Quartapelle, 'Finite element method for non-linear hyperbolic problems', *J. Comput. Methods Appl. Mech. Eng.*, **52**, 817–845 (1985).
10. K. W. Morton, 'Generalized Galerkin methods for hyperbolic problems', *J. Comput. Methods Appl. Mech. Eng.*, **52**, 847–871 (1985).
11. A. J. Baker and J. W. Kim, 'A Taylor weak-statement algorithm for hyperbolic conservation laws', *Int. j. numer. methods fluids*, **7**, 489–520 (1987).
12. R. Schreiber and H. B. Keller, 'Driven cavity flows by efficient numerical techniques', *J. Comput. Phys.*, **49**, 310–333 (1983).